Effect of mechanical activation of reagents' mixture on the high-temperature synthesis of Al_2O_3–TiB_2 composite powder

R. Taherzadeh Mousavian · S. Sharafi ·
M. R. Roshan · M. H. Shariat

Abstract A powder mixture of $Al/TiO_2/H_3BO_3 = 10/3/6$ in molar ratio was used in this study to form the Al_2O_3–TiB_2 ceramic composite via thermite reactions (combustion synthesis). As no combustion synthesis occurred for an unmilled sample in a furnace, the mixture was milled in a planetary ball-mill for various milling times, and the as-milled samples were in situ synthesized in the furnace at a heating rate of 10 °C/min. The differential scanning calorimetry (DSC) measurements were performed with the same heating rate on the unmilled and the as-milled samples to evaluate the influences of the milling on the mechanisms and efficiencies of reactions. Although no combustion synthesis occurred for the unmilled sample in the furnace, two exothermic peaks were detected in its DSC curve after the melting of the Al. For the as-milled samples, significant changes revealed in the DSC curves, suggest that the milling process before the combustion synthesis changed the mechanisms and efficiencies of reactions. In addition, the intensity and the temperature of the exothermic peaks in the DSC curves changed by increasing the milling time. According to the XRD analyses, by enhancing the milling time, the purity of the final products would increase, confirming that the efficiency of the reactions increased. Finally, the microstructures of the as-milled and as-synthesized samples were examined by a SEM, and it was shown that the morphology of the reactant powders was altered by increasing the milling time.

Introduction

Transition metal diborides like TiB_2 are important materials for light armors, nozzles, coatings, cutting tools, wear parts, and high-temperature applications due to their superior properties such as high-melting points (above 3,000 °C), relative low density (e.g. 4.5 g/cm^3 for TiB_2), high hardness, good thermal and electrical conductivity, and excellent wear resistance. The addition of Al_2O_3 to these metal diborides further improves their fracture toughness, flexural strength, sinterability, and impact resistance, which renders the $Al_2O_3^-$ reinforced diboride composites a promising candidate for a variety of applications including cutting tools, wear-resistant parts, heat exchangers, and high-temperature structural materials [1, 2].

The combustion synthesis (CS) has the advantages of low energy requirement, short processing time, simplicity of facilities, formation of high-purity products, and stabilization of metastable phases [2, 3]. Recently, Deqing [1] fabricated an Al_2O_3–TiB_2 in situ composite by using boric acid instead of B_2O_3 as a boron source, reaction (1), which is economically and technologically more attractive in synthesizing the Al_2O_3–TiB_2 ceramic composite.

$$10Al + 3TiO_2 + 6H_3BO_3 \rightarrow 5Al_2O_3 + 3TiB_2$$
$$+ 9H_2O, \quad \Delta H_{(298)} = -2518.9 \, (\text{kJ/mol}). \quad (1)$$
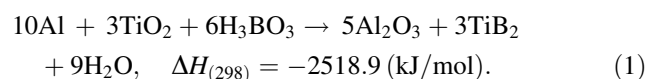
Despite the high-heat content of the composition, usually it is extremely difficult to initiate combustion in the initial

R. T. Mousavian (✉) · S. Sharafi
Materials Science and Engineering Department, Shahid Bahonar University of Kerman, Kerman, Iran
e-mail: rtaher1898@gmail.com

M. R. Roshan · M. H. Shariat
Materials Science and Engineering Department,
School of Engineering, Shiraz University, Shiraz, Iran

samples that were not subjected to the milling process, even if a high-temperature primer is used. Therefore, the milling process is usually needed, even for a few minutes, to assist the combustion synthesis. The milling process before CS usually changes the energy level and the morphology of the reactants, increases the contacting surface area between the reactants, and increases the intensity and the efficiency of the CS reaction(s). These combined effects significantly alter the reaction(s) kinetics and the resulting phases. The other possible effect of milling is changing the reaction(s) temperature in the CS process. Therefore, the milling process may change the thermal behavior of the mixed powders, thermodynamically and kinetically [4–6].

Differential scanning calorimetry (DSC) is a convenient method for investigating chemical thermodynamics and formal kinetic descriptions of physico-chemical processes, and many researchers have utilized this technique to study thermal behavior during milling or combustion synthesis, crystallization, phase transformation, and so on [7–11]. The present research has been undertaken to study the effects of milling time on the mechanisms and efficiencies of reactions in the Al–TiO$_2$–H$_3$BO$_3$ system, using DSC, XRD, and SEM analyses.

Experimental procedures

Boric acid (mean particle size below 80 μm, purity 99%), titanium dioxide (anatase, with a submicron average particle size of 0.6 μm, purity of 99.5%), and reducing agent aluminum (mean particle size below 30 μm, purity of 99.5%) were used as reagents for the CS of TiB$_2$–Al$_2$O$_3$ ceramic composite.

The constituent powders, which were prepared with designed stoichiometry according to reaction (1), were exposed to the milling process in a ball-mill. Four samples (marked by S$_1$ to S$_4$) were ball-milled for 5, 10, 15, and 25 h, respectively, with a rotating speed of 250 rpm. The milling process was performed under argon atmosphere (with purity of 99.9%) by using a Fritsch planetary ball-mill with an alumina vial and a blend of alumina balls (10 and 20 mm diameters). The milled powders were then oven-dried at 90 °C for 3 h and were passed through a 100-mesh sieve. The powder mixtures were uniaxially pressed without a binder at 400 MPa into a cylindrical compact of 2 cm diameter and 1 cm height to approximately 60% relative density, and the billets were in situ synthesized in a furnace at a heating rate of 10 °C/min. The ignition temperature during combustion synthesis in the furnace for the as-milled samples was recorded.

The physico-chemical changes in the Al–TiO$_2$–H$_3$BO$_3$ thermite system during heating of the unmilled and as-milled samples were investigated using a simultaneous TG/DSC measurement using a Netzsch STA 409 (Germany) analyzer with a maximum working temperature of 1,500 °C to study the effects of milling time on the mechanisms and efficiencies of the reactions. The TG/DSC experiments utilized high-purity corundum as a reference. Powder samples of ≈30 mg were loaded and pressed into an alumina crucible, which will not react with the reactants, and heated up in an inert argon atmosphere at the rate of 10 °C/min, followed by cooling down at the same rate for all the samples. The last exothermic peak temperature for the as-milled samples in the DSC curves was compared with the recorded ignition temperature in the furnace.

The as-milled and as-synthesized samples were exposed to X-ray analysis (Bruker's D8 advance system, Germany) using Cu K$_\alpha$ ($\lambda = 0.15405$ nm) radiation, and based on the DSC curves of the as-milled samples, intermediate products, which were formed after the first exothermic peak, were subject to XRD analysis for phase determination. The microstructures of the as-milled and as-synthesized samples were studied using a scanning electron microscope (SEM, Camscan mv2300).

Results and discussion

As no combustion synthesis occurred for the unmilled sample in the furnace, the mixture was milled for different milling times. Figure 1 shows the XRD patterns of the samples, which were milled up to 15 h. As can be seen in this figure, increasing the milling time did not change the present phases, indicating that no reaction took place during the milling process, and only the intensity of boric acid peaks decreased slightly. The intensity depression of the boric acid peaks might be due to an increased temperature above 120 °C in the microscopic scale caused by increasing the milling time, leading to the thermal decomposition of boric acid, and the moisture removal.

Besides the reactants peaks, the peaks of the alumina and the Al–Ti intermetallic phases are detected in the XRD pattern of the sample S$_4$ that was milled for 25 h (see Fig. 2). This indicates that further milling up to 25 h led to the reaction between Al and TiO$_2$ to form alumina (reaction 2) and intermetallic phases of Al–Ti during the milling process.

The DSC trace of the unmilled sample shows that the reactions occurred in two steps (see Fig. 3). The endothermic peaks that appeared between 120 to 170 °C and at about 300 °C are due to the thermal decomposition and evaporation of boric acid, respectively. A sharp endothermic peak at about 660 °C corresponds to the melting of the Al. As shown in Fig. 3, there is no evidence of any sharp peak related to the melting of B$_2$O$_3$, which was expected to

Fig. 1 X-ray phase analyses of the as-milled samples: **a** S_1, **b** S_2, and **c** S_3
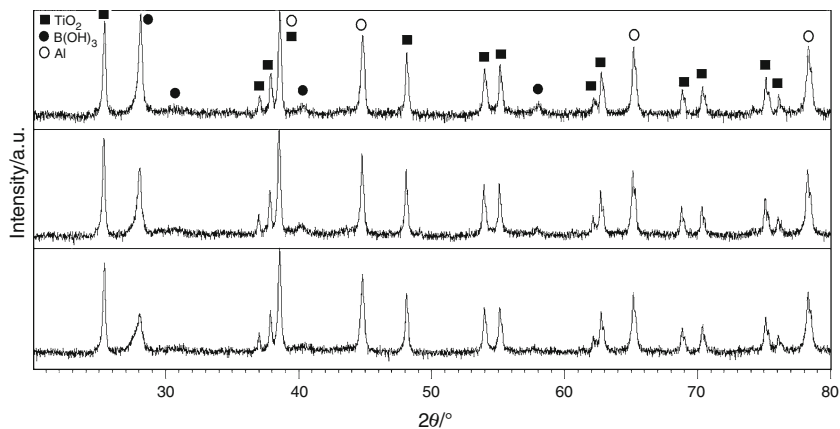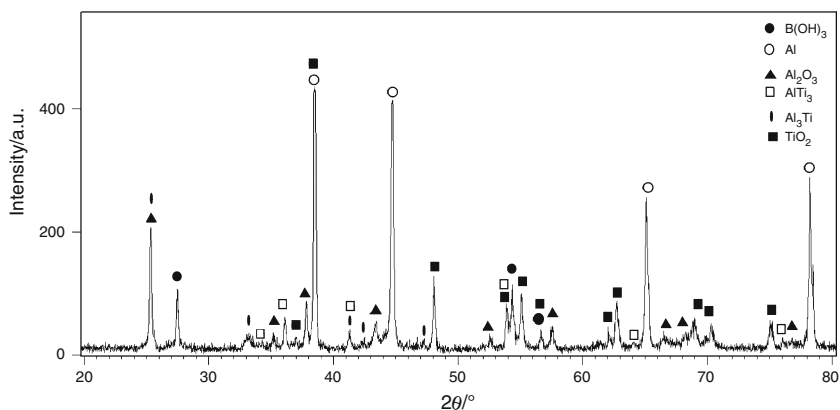

**Fig. 2** X-ray phase analysis of the as-milled sample S_4

be detected at about 450 °C. Weimin et al. [12] and other researchers [3, 13, 14] also did not report the detection of a B_2O_3 melting peak. To the best of our knowledge, no reason has yet been proposed to explain why the sharp melting peak of B_2O_3 could not be detected in DSC measurements. According to Stolen [15], the crystallization of the stable crystalline phase is hindered due to an activation barrier caused by the surface energy of the crystal nuclei. In some cases like B_2O_3, stable crystals barely form.
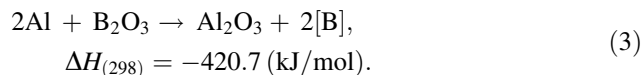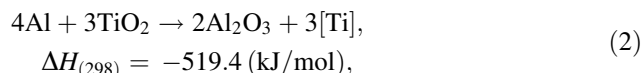
Therefore, a sharp visible melting peak could not be detected during heating in a calorimeter. Based on this fact, boron oxide usually has low intensity peaks in the X-ray phase analysis in comparison with the Al and TiO_2.

As shown in Fig. 3, two subsequent exothermic peaks are observed after the melting peak of the Al. Based on the combustion synthesis mechanism of the Al_2O_3–TiB_2 composite proposed in previous studies [1, 2, 14], it can be concluded that the first exothermic peak, which appears at
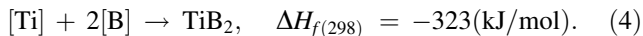
Fig. 3 The TG/DSC curves of the unmilled sample
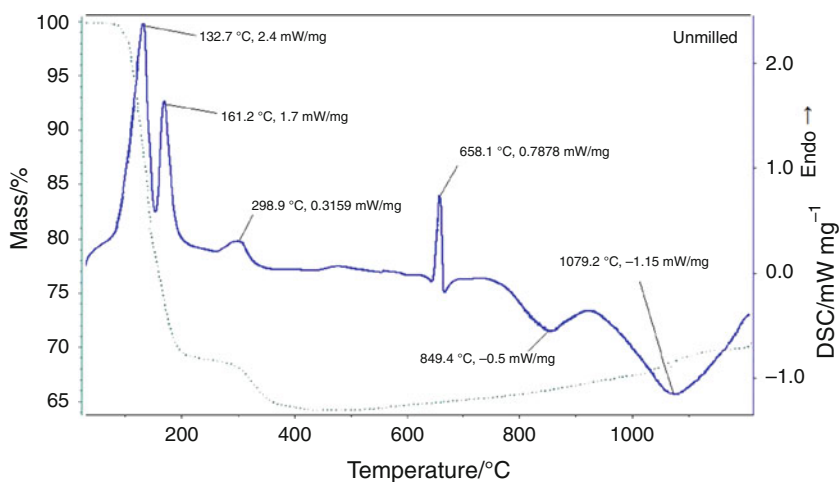
about 849 °C, emanated from the occurrence of thermite reactions (2) and (3).

$$4Al + 3TiO_2 \rightarrow 2Al_2O_3 + 3[Ti],$$
$$\Delta H_{(298)} = -519.4 \,(\text{kJ/mol}),$$
(2)

$$2Al + B_2O_3 \rightarrow Al_2O_3 + 2[B],$$
$$\Delta H_{(298)} = -420.7 \,(\text{kJ/mol}).$$
(3)

The last exothermic peak, which was revealed at about 1,079 °C, represents the formation of the TiB_2, according to reaction (4).

$$[Ti] + 2[B] \rightarrow TiB_2, \quad \Delta H_{f(298)} = -323(\text{kJ/mol}). \quad (4)$$

In the Lu et al. study [16], it was reported that in the Al–B_2O_3–TiO_2 system, the Al_2O_3 is obtained at first, thermodynamically, and the Ti and B atoms can be freed by the formation of the Al_2O_3. Subsequently, the free Ti and B atoms react with the Al and each other to form the Al–B, Al–Ti, and Ti–B interphases compounds. However, Gibbs free energy of TiB_2 formation is the lowest among the other interphases compounds, meaning that TiB_2 is the most stable phase for all temperature ranges, and, therefore, after the alumina, TiB_2 will be produced during the last exothermic peak. Based on the assumption that the Ti and B atoms are reduced simultaneously, by the thermite reactions, TiB_2 can be formed by a direct reaction between reduced Ti and B (reaction 4).

The TG/DSC curves of the as-milled samples are shown in Fig. 4. This figure clearly demonstrates that the milling process deeply affected the mechanisms and efficiencies of the reactions. In contrast to Fig. 3, the peak corresponding to the evaporation of the boric acid at about 300 °C cannot be detected for the as-milled samples, indicating that no boric acid remained after thermal decomposition for these samples. Moreover, an extra exothermic peak was revealed just

before the melting point of the Al for samples S_1 to S_3 (Fig. 4a–c), while it was not detected in the DSC trace of the unmilled sample. As mentioned in the "Experimental procedures" section, in order to clarify the nature of this peak, an interrupted DSC experiment was conducted for the sample S_1 which was heated up to a temperature just below the melting point of the Al, and the heated sample was analyzed by XRD. The presence of Al–Ti intermetallic compounds in the pattern of X-ray diffraction phase analysis (Fig. 5) confirmed that this exothermic peak was mainly caused by the reduction reaction of TiO_2. This shows that, due to the milling process the interfacial area increased significantly between the Al and the fine TiO_2 powders. Therefore, reaction (2) took place for the as-milled samples at lower temperatures below the melting of the Al. Yeh et al. [2] and Ma et al. [17] have reported that the reduction reaction of TiO_2 took place before that of B_2O_3, whereas the particle size of TiO_2 was much smaller than that of B_2O_3. Tekmen et al. [14] have reported only two exothermic peaks after the Al melting, which corresponded to the formation of Al_2O_3 (due to thermite reactions) and TiB_2, respectively, since in their work the size of the TiO_2, B_2O_3, and Al powders were close to each other and no exothermic peak was detected before the melting of the Al.

With the same particle size of TiO_2 and B_2O_3, it seems that the reduction reaction of B_2O_3 might take place before that of TiO_2 because of the liquid phase formation of B_2O_3. However, as indicated before, the enthalpy of reaction (2) is more negative than that of reaction (3). Ying et al. [18] have reported that the onset reaction temperature between Al and TiO_2 completely depends on the interfacial area between the reactants. At the beginning of the milling treatment, the Al particles easily undergo plastic deformation and gradually encapsulate the TiO_2 and H_3BO_3 particles, which are harder and more brittle. As the size of

Fig. 4 The TG/DSC curves of the as-milled samples: a S_1, b S_2, c S_3, and d S_4
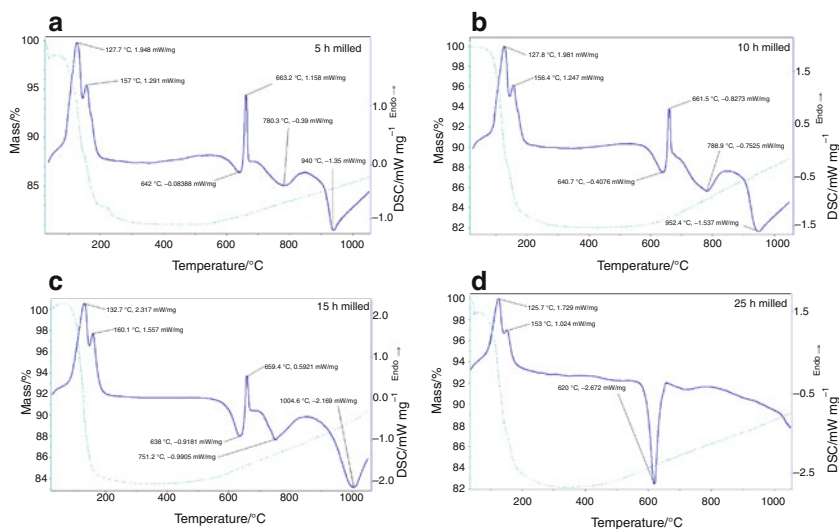
TiO_2 particles is much smaller than that of boric acid in our work, TiO_2 particles are covered by Al much more than boric acid particles. However, due to the melting of B_2O_3 and the effect of capillary phenomenon, the reduction of B_2O_3 may take place. Nevertheless, because of their small amounts, the reduced [B] and its intermetallics could not be detected by XRD. For the unmilled sample, there is no significant difference in the interfacial area between the Al with TiO_2 and B_2O_3, and the metal oxides were reduced during the first exothermic peak after the melting of the Al. Also, due to the very low interface area between the reactants, higher temperature and more time were required for the metal oxides to be reduced.

The second exothermic peak after the melting of the Al mainly corresponds to the reduction reaction of B_2O_3. Moreover, it should be considered that the reduced [Ti] formed by reaction (2), may react with B_2O_3 to form TiO_2, according to reaction (5).

$$3Ti + 2B_2O_3 \rightarrow 3TiO_2 + 4B,$$
$$\Delta H_{f(298)} = -305 \, (kJ/mol). \tag{5}$$
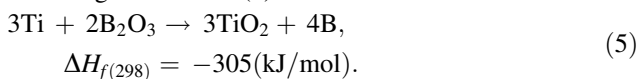
According to Fig. 5, the XRD pattern included considerable amounts of the remained TiO_2, which shows that not all of the TiO_2 powders reacted with the Al during the first exothermic peak. This remained TiO_2 and the TiO_2 that was formed by reaction (5) will react with the Al during the second exothermic reaction. Like the unmilled DSC trace, the last exothermic peak in the DSC curves of the samples S_1 to S_3 corresponds to the formation of TiB_2. For the as-milled samples, the Ti and B atoms were not reduced at the same time. Therefore, intermetallic phases of Al–Ti and Al–B can be formed due to reactions between the Ti and Al below and after the melting of the Al, and between the B and Al mainly after the melting of the Al. Thus, for these samples, titanium diboride was most probably formed during the possible reactions between Al–Ti and the Al–B interphases, e.g. by reaction (6).

$$Al_3Ti + AlB_2 \rightarrow TiB_2 + 4Al,$$
$$\Delta G_T^\circ = -74701 + 5T \, (kJ/mol \, k). \tag{6}$$
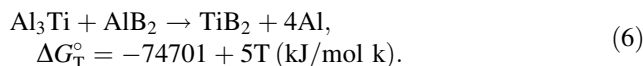
As can be seen in Figs. 3 and 4, by increasing the milling time, the reaction temperature and intensity have changed significantly. From thermodynamic and kinetics points of view, the milling process effectively lowers the activation barriers for reactions. Therefore, it is expected that the reactions' temperature should decrease by increasing the milling time. Figure 4a shows the DSC trace of the sample S_1, which was milled for 5 h. As this figure shows, the last two exothermic reactions took place at temperatures about 70 and 140 °C below those of the unmilled sample. However, as Fig. 4b and c show, the exothermic reactions temperature did not decrease with increasing the milling time from 5 to 15 h, which is not in agreement with our expectations. This can be justified by using SEM micrographs of the as-milled samples. According to the SEM micrographs (Fig. 6), the milling up to 5 h did not make any considerable change in the particle size and morphology of the powders. Figure 6a reveals the presence of the big particles (>45 μm) with very small particles (<1 μm) beside each other. However, by increasing the milling time from 5 to 15 h, the particle size of the as-milled powders increased dramatically. Thus, the diffusion from the center of the particles will take more time and a higher temperature due to the increase in the particle size (Fig. 6b). Furthermore, by increasing the particle size, the interfacial area between the particles would decrease. In addition, it is obvious that the nearly spherical-like morphology changed to a flake-like morphology during the milling process. The spherical-like morphology has a much greater interfacial area than the flake-like morphology. Our visual examinations show that boric acid would exhibit adherent behavior when it is held in a temperature above 120 °C. In fact, due to the increased temperature caused by further ball-to-ball and ball-to-powder collisions after 5 h, the boric acid would

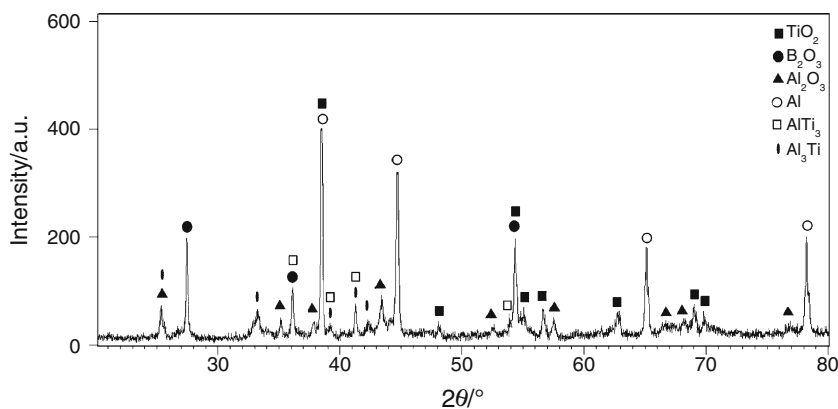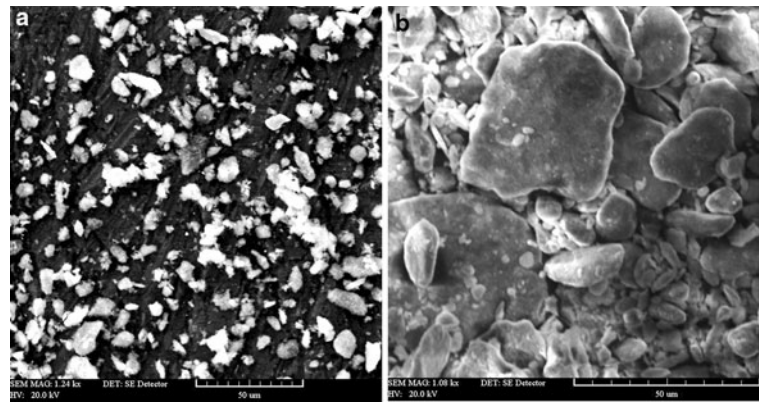**Fig. 5** The X-ray phase analysis of the sample S_1 heated up to 660 °C

Fig. 6 SEM microstructures of the as-milled samples: **a** S$_1$, and **b** S$_3$


decompose, and the water molecules cause agglomeration of the particles and severe adhesion. Therefore, despite an increase in the energy level of the reactants, higher temperatures were needed for the samples S$_2$ and S$_3$ to form TiB$_2$.

On the other hand, the DSC results showed that by applying the milling process, the exothermic peaks' intensity of the samples increased significantly. As depicted in Figs. 3 and 4, the energy released by the unmilled sample is lower than that for the as-milled samples, suggesting the efficiency of the reactions is low. As no combustion synthesis took place for the unmilled sample in the furnace, it can be concluded that the reactions might not take place in the entire unmilled sample, due to the insufficient mixing of the reactants, and very low interfacial area between the reactants. However, for the as-milled samples, because of the higher interfacial area and higher mixing (kinetically), and the higher energy level of the reactants (thermodynamically), the reactions took place more intensively, and the CS took place for them in the furnace. In these samples, each phase within a particle could be thought of as being surrounded with the other phases, allowing diffusion in all directions simultaneously

and not just in the direction of the contact points, as in the unmilled sample. In fact, by increasing the milling time, more Al surface comes into intimate contact with TiO$_2$ and H$_3$BO$_3$, thus enhancing the efficiency of the reactions. The X-ray phase analysis of the as-milled samples, which was in situ synthesized by the thermal explosion mode of combustion synthesis in the furnace, confirmed that by increasing the milling duration, the efficiency of the reactions would increase. In fact, despite the agglomeration of the particles, the homogeneity of the phases would not decrease, as the phases had been homogenized after 5 h. Figure 7 shows that the final products of sample S$_1$ are composed of TiB$_2$, Al$_2$O$_3$, and considerable amounts of Al and TiO$_2$. Due to the oxide coating on the Al powders, a small amount of Al remained unreacted after combustion synthesis, and consequently not all the metal oxides could be reduced. However, by increasing the reactions' intensity, the amounts of Al and TiO$_2$ presented in the products decreased gradually. The alumina oxide film on the Al particles acts as a diffusion inhibitor during sintering and/ or combustion synthesis and can be suitably broken during the milling process. Therefore, a depression in the intensity of the reactants' peaks (Fig. 7) due to the milling up to

Fig. 7 The XRD phase analyses of as-synthesized samples: (*a*) S$_1$, (*b*) S$_2$, (*c*) S$_3$, and (*d*) S$_4$
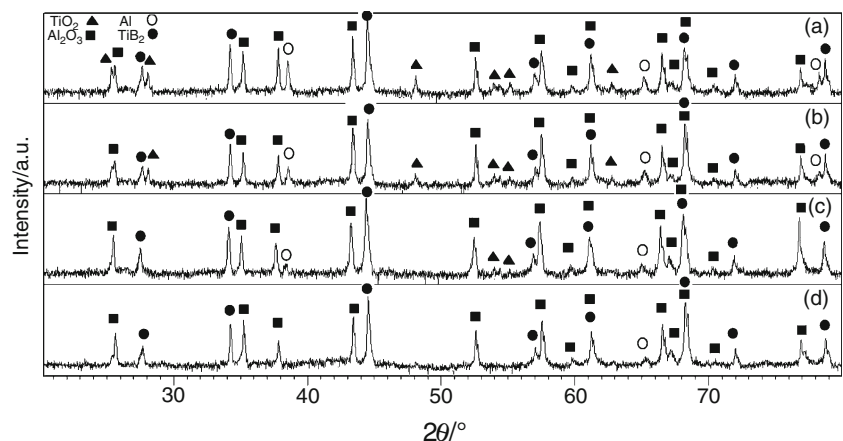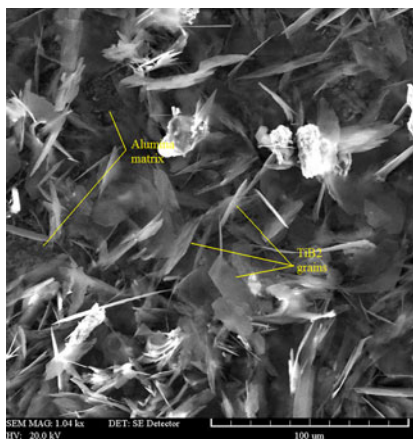
Fig. 8 A typical SEM microstructure of the sample S_1, which is in situ synthesized in a furnace

25 h can be justified by the destruction of the protective oxide film on the Al particles and the increased intensity of the reactions thermodynamically, leading to the liberation of more heat and higher temperature.

The DSC curve of the sample S_4 only showed an exothermic peak at about 620 °C (Fig. 4d), suggesting that the milling process up to 25 h significantly affected the combustion synthesis mechanism since the ignition combustion temperature reduced to 620 °C (below the melting point of the Al). No melting peak of the Al was detected, indicating that the Al has been consumed completely during this exothermic reaction. Hence, the combustion synthesis process occurred in one step for this sample. This is because of the fact that the thermite reaction (2) took place to some extent during the milling process, and a considerable amount of heat was released as the alumina formed. This liberated heat may dissociate the boric acid and reaction (3) could take place during the milling process. Moreover, 25 h milling can enhance the energy of the reactants to a high level. Therefore, during heating in the calorimeter at 620 °C, all the exothermic reactions took place at the same time.

The ignition temperature for the as-milled samples during combustion synthesis with a heating rate of 10 °C/min in the furnace was visually obtained to be 903, 911, 938, and 595 °C. These results are in good agreement with the results of the DSC measurements. Our visual examinations showed that during heating, the as-milled samples appeared reddish yellow in color after about 880 °C for the samples S_1 to S_3. In fact, due to the occurrence of thermite reactions, a considerable heat will be liberated, and finally, the thermal explosion will occur during the last exothermic peak of the DSC curves, when TiB_2 forms. It should be considered that the samples in the furnace were uniaxially pressed to a high-relative density, while the samples that

were heated in the calorimeter were only pressed under a very low pressure. This may be the reason for the differences of the obtained ignition temperatures. Additionally, the weight of the sample might affect the ignition temperature. As reported, a significant reduction (more than 300 °C) in the ignition temperature was observed for sample S_4. In fact, before any change in the color of the sample, the thermal explosion occurred for this sample more intensively below 600 °C in the furnace, indicating that in spite of the agglomeration of the particles, the energy level of the reactants increased considerably during the milling process, even about the activation energy that is needed for the reactions. In fact, for the samples S_1 to S_3, in addition to the external heat that is given to the samples during heating in the furnace and the calorimeter, the heats of reactions (2 and 3) are needed for the occurrence of the reaction (4 or 6). While, for the sample S_4, only an external heat is needed for the occurrence of the reaction (4 or 6), and all the reactions take place at the same time and temperature.

A typical SEM microstructure of the porous as-synthesized sample S_1 is shown in Fig. 8, in which hexagonal flake-like TiB_2 grains formed beside the solidified alumina matrix. In fact, the final combustion temperature is above the melting of the alumina [1]. Therefore, the alumina phase that is produced at the first step of combustion synthesis is melted and the TiB_2 phase is in situ synthesized beside the alumina.

Conclusions

In this study, the $Al–TiO_2–H_3BO_3$ was used for the combustion synthesis of the $Al_2O_3–TiB_2$. As no combustion synthesis occurred for the unmilled sample, the milling process was applied to aid the combustion synthesis. By means of DSC, XRD, and SEM analyses, the effects of milling time on the mechanisms and efficiencies of reactions were investigated. From the DSC measurements, the law of physico-chemical change in this chemical system for the as-milled samples can be summarized as: loss of absorbed water → melting of the B_2O_3 → $3TiO_2$ (s) + $4Al(s) = 3Ti(s) + 2Al_2O_3(s)$ → formation of the Al–Ti intermetallic compounds → melting of Al → $3TiO_2$ (s) + $4Al(l) = 3Ti(s) + 2Al_2O_3(s)$ and $B_2O_3(l) + Al(l) = 2B(s) + Al_2O_3(s)$ → formation of the Al–Ti and Al–B intermetallic compounds → $Ti(s) + 2B(s) = TiB_2(s)$. For the unmilled sample, after the melting of the Al, the thermite reactions took place initially, and finally, during the last exothermic reaction titanium diboride formed. The other significant conclusions can be drawn as follows:

1. The Al_2O_3–TiB_2 in situ composite can be fabricated by using boric acid instead of the B_2O_3 as a boron source.

2. According to X-ray phase analyses no exothermic reaction took place for the samples milled up to 15 h.

3. Short milling time up to 5 h will decrease the temperature of the combustion synthesis reactions. However, due to the agglomeration of the particles, caused by a prolonged milling time up to 15 h, and the depression in the interfacial area between the particles, the temperature of the reactions increased.

4. An important influence of the milling is a considerable enhancement of the reactions intensity during combustion synthesis, demonstrating an increase in the efficiency of the reactions, resulting in the elimination of the reactants in the final products due to the destruction of the oxide layer during the milling process.

5. Prolonged milling up to 25 h changed the formation mechanism of the Al_2O_3–TiB_2 in situ composite, from 3 steps to one step.

6. As a result of prolonged milling, the morphology of the particles changed from nearly a spherical-like morphology to a flake-like morphology, resulting in a decrease in the contact area between the particles.

7. There are good agreements between the temperatures of the last exothermic peaks in the DSC curves of the as-milled samples with the ignition temperatures observed in the furnace.

References

1. Deqing W. Effects of additives on combustion synthesis of Al_2O_3–TiB_2 ceramic composite. J Eur Ceram Soc. 2009;29: 1485–92.

2. Yeh CL, Li RF. Formation of TiB_2–Al_2O_3 and NbB_2–Al_2O_3 composites by combustion synthesis involving thermite reactions. Chem Eng J. 2009;147:405–11.

3. Mishra SK, Das SK, Ramachandrarao P, Belov DY, Mamyan S. Synthesis of zirconium diboride–alumina composite by the self-propagating, high-temperature synthesis process. Metall Mater Trans A. 2003;34:1979–83.

4. Korchagin MA, Bokhonov BB. Combustion of mechanically activated 3Ti + 2BN mixtures. Combust Explos Shock Waves. 2010;46(2):170–7.

5. Kovalev DY, Kochetov NA, Ponomarev VI, Mukasyan AS. Effect of mechanical activation on thermal explosion in Ni–Al mixtures. Int J SHS. 2010;19:120–5.

6. Korchagin MA, Dudina DV. Application of self-propagating high-temperature synthesis and mechanical activation for obtaining nanocomposites. Combust Explos Shock Waves. 2007;43(2):176–87.

7. Stojanovic BD, Marinkovic ZV, Brankovic GO, Fidanevska E. Evaluation of kinetic data for crystallization of TiO_2 prepared by hydrolysis method. J Therm Anal Calorim. 2000;60:595–604.

8. Sorescu M, Xu T. The effect of ball-milling on the thermal behavior of anatase-doped hematite ceramic system. J Therm Anal Calorim. 2010. doi:10.1007/s10973-010-1016-1.

9. Wiezorek-Ciurowa K, Gamrat K, Sawlowicz Z. Characteristics of $CuAl_2$–Cu_9Al_4/Al_2O_3 nanocomposites synthesized by mechanical treatment. J Therm Anal Calorim. 2005;80:619–23.

10. Wiezorek-Ciurowa K, Gamrat K. NiAl/Ni_3Al–Al_2O_3 composite formation by reactive ball milling. J Therm Anal Calorim. 2005;82: 719–24.

11. Patoya ML, Granier JJ. The effect of slow heating rates on the reaction mechanisms of nano and micron composite thermite reactions. J Therm Anal Calorim. 2006;85(1):37–43.

12. Weimin W, Zhengyi F, Hao W, Runzhang Y. Chemistry reaction processes during combustion synthesis of B_2O_3–TiO_2–Mg system. J Mater Process Technol. 2002;128:162–8.

13. Khanra AK. Reaction chemistry during self-propagating high-temperature synthesis (SHS) of H_3BO_3–ZrO_2–Mg system. Mater Res Bull. 2007;42:2224–9.

14. Tekmen C, Tsunekawa Y, Okumiya M. In situ TiB_2–Al_2O_3 formed composite coatings by atmospheric plasma spraying: influence of process parameters and in-flight particle characteristics. Surf Coat Technol. 2009;203:1649–55.

15. Stølen S, Grande T, Allan NL. Chemical thermodynamics of materials: macroscopic and microscopic aspects. 1st ed. Nottingham: Wiley; 2004.

16. Lu L, Lai M, Su Y, Teo HL, Feng CF. In situ TiB_2 reinforced Al alloy composites. Scripta Mater. 2001;45:1017–23.

17. Ma ZY, Tjong SC. In situ ceramic particle-reinforced aluminum matrix composites fabricated by reaction pressing in the TiO_2 (Ti)–Al–B (B_2O_3) systems. Metall Mater Trans A. 1997;28: 1931–42.

18. Ying DY, Zhang DL, Newby M. Solid-state reactions during heating mechanically milled Al/TiO_2 composite powders. Metall Mater Trans A. 2004;35:2115–25.